Available online at www.sciencedirect.com

ScienceDirect

Energy Procedia 4 (2011) 4387–4394

Energy Procedia

www.elsevier.com/locate/procedia

GHGT-10

Permeability alteration due to salt precipitation driven by drying in the context of CO_2 injection

Y. Peysson, B. Bazin, C. Magnier, E. Kohler, S. Youssef

IFP Energies Nouvelles, 1-4 avenue de Bois Préau, 92852 Rueil-Malmaison Cedex - France

Abstract

Injection of large quantities of CO_2 for underground geological storage in shallow or deep saline aquifers will lead to a strong water desaturation of the near wellbore because of drying mechanisms. Even the capillary trapped water can be removed by thermodynamical transfert of water vapour in the CO_2 phase. In this context, drying mechanisms can precipitate the salt present in the aquifer and then lead to injectivity alteration.

In this study, we investigated experimentally the alteration of permeability induced by drying of brine in porous media for different rocks and different brines. Initial characterization on four types of dry rock sample representative of storage rocks was performed including gas permeability and porosity measurements. Two sandstones and two carbonate rocks of large and medium permeability were tested to evaluate the effect of rock type and initial permeability on the injectivity alteration. Each sample was fully saturated with a brine of different salt composition (KCl, NaCl and Keuper brine, a mixture of salt representative of the Paris Basin brine aquifer) and different salinity up to 250 g/L. The samples were then completely dried in an oven at controlled temperature and with vapour evacuation. Return gas permeabilities were then measured on each sample after full drying.

Local analysis at the pore scale, with scanning electron microscopy and micro-Xray scanner have been done to observe the type of flow obstruction and the spatial repartition of the salt deposit in the pore matrix.

"Keywords: Salt precipitation ; permeability alteration ; drying effects"

1. Introduction

Shallow or deep saline aquifers are potential interesting sites for geological storage of CO_2 because their storage capacities, in terms of volume, fit the order of magnitude of a consequent amount of the annual world CO_2 emissions, and because of their high salinity they will not be used for drinkable water. Injection of large quantities of dry CO_2 in such geological objects will likely lead to a total water desaturation of the near wellbore because even the capillary trapped water will be removed by thermodynamical transfert of water vapour in the CO_2 phase. In this context, drying mechanisms can precipitate the salt present in the aquifer and then lead to injectivity alteration. The number of injecting wells for carbon underground geological storage will be limited mainly due to the economy of the technology. So, injectivity issues are essential because a high level of carbon dioxide flow rate has to be maintained for a long time period (typically 50 years).

Drying in porous media has been studied mainly in the diffusive regime were the water vapour escapes from the

doi:10.1016/j.egypro.2011.02.391

rock structure by diffusion [1]. The injection of CO_2 in porous media has raised the interest of drying by convection where the water vapour is evacuated by the gas flow through the porous structure. Recent works, essentially numerical simulations, have been done to evaluate the risk of salt deposition in the case of underground geological storage. Two phase Darcy flow models were used to calculate the distribution of phases saturation in time [2-4]. Some experimental works have been done [5-6] but essentially on drying mechanisms. Complementary experiments are still needed to clarify the main mechanisms involved in the case of coupled effects, drying and precipitation and to validate the model hypothesis.

The objective of this work was to study the permeability alteration due to salt precipitation induced by drying in controlled conditions to be able to have the trend of permeability decrease with the solid salt saturation.

2. Experiments

2.1. Rocks

Four types of rocks representative of storage sites were employed. Two sandstones and two carbonate quarry rock blocks were selected due to their good level of homogeneity at the core scale. Samples of diameter 23mm and length 93mm were cored from the four blocks and dried. The initial average properties of the samples are given in Table 1.

Rock type	*Average Permeability* K_g^i(mD)	*Average Porosity* ϕ_0
Vosges Sandstone 1	120	21.4
Vosges Sandstone 2	2900	21.6
Lavoux limestone 1	4	24.6
Lavoux limestone 2	620	26.7

Table 1 : Rock type properties

All selected quarry blocs were characterized by X-ray diffractometry. The Lavoux limestone are essentially calcite with some traces of quartz. The Vosges Sandstone blocs are 70% quartz, 20% microcline and about 10% of a mixture of clays : mica, kaolinite and illite.

2.2. Fluids

Three different brines were prepared to evaluate the type of salt effect: Sodium Chloride NaCl ; Potassium Chloride KCl and a mixture of salt representative of the Paris Basin brine, the Keuper brine [7] (Composition : KCl 4.12 g/L ; $MgCl_2$,$6H_2O$ 5.23 g/L ; $CaCl_2$,$2H_2O$ 22.00 g/L ; NaCl 139.33 g/L; Na_2SO_4 0.52 g/L). The initial salt concentration C_i of NaCl and KCl varied in the experiments in a large range from 0 to 250 g/L.

2.3. Methodology

For each sample, the same methodology was applied. The initial dry sample was sleeved and loaded in a core holder and an effective confining stress was applied. Initial gas permeability K_g^i was measured at ambient conditions with Nitrogen step flows. The sample was then vacuumed, fully saturated with the brine and finally placed in an oven and dried at the temperature of 60°C and with vapour evacuation. The level of saturation was controlled by regular mass measurements. The sample was loaded again in the core holder and final gas permeability K_g^f was measured in the same conditions than K_g^i.

3. Results

The permeability alteration is defined as the ratio of gas permeability after drying with the initial one K_g^f/K_g^i. The alteration is represented versus the initial brine concentration C_i for KCl and the four types of rocks in Figure 1.

3.1. Influence of rock type

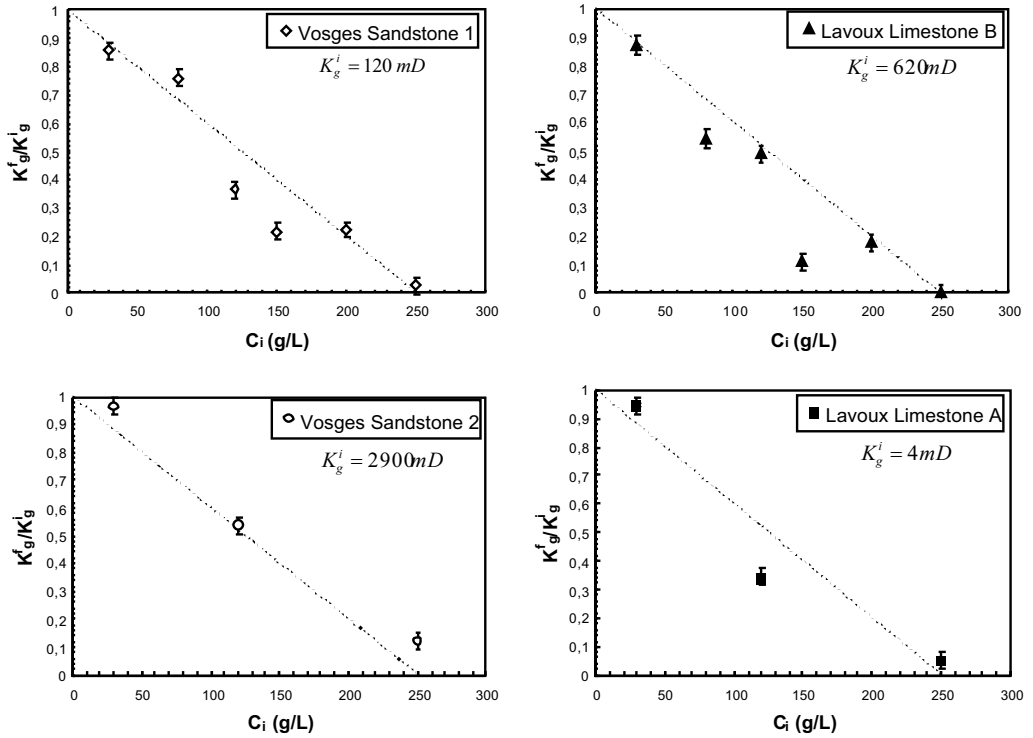

Figure 1 : Permeability alteration versus salt initial concentration C_i for the four type of samples and KCl.

The permeability alteration decreases with the initial salt concentration C_i and is nearly total for C_i = 250 g/L. A linear trend has been added on Figure 1.

3.2. Influence of salt

Figure 2 represents the permeability alteration for the three used salts with the Vosges Sandstones 1. The repeatability is also represented. The experimental methodology has been repeated with 4 different samples with the same brine in the same conditions. The results are in closed agreements.

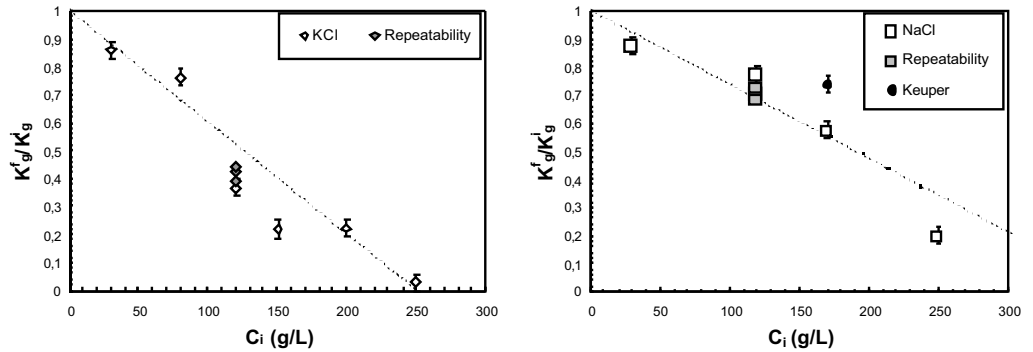

Figure 2 : Permeability alteration versus salt initial concentration for the three types of brines and the Vosges Sandstone 1.

The type of salt influences clearly the alteration. We do observe the same linear trend, but the decrease is lower in the case of NaCl. Keuper brine is composed in majority of NaCl and the measured alteration is closed to the NaCl curve.

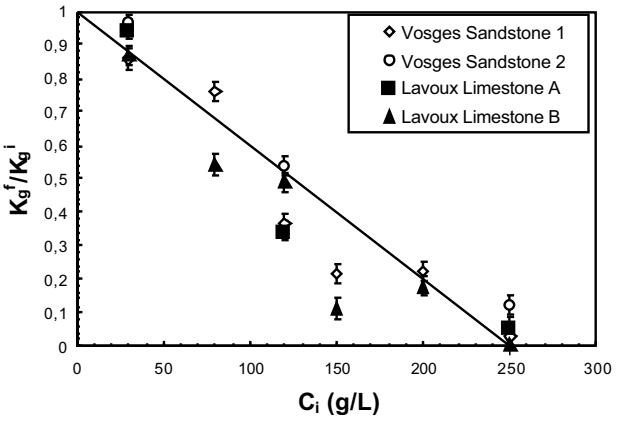

Figure 3 : Permeability alteration versus salt initial concentration for the four types of rocks and KCl.

In Figure 3, the alteration of four rock types is represented in the case of KCl. A remarkable result is that the previously observed linear trend is the same for all four experiments: the alteration depends only slightly on rock type and initial permeability.

3.3. Alteration model

To explain the trend observed in the experiments, we calculated the permeability alteration based on a volume balance model and a representation of the permeability by parallel capillary tubes. This simple representation has only two parameters, the density of tubes N/A (N: number of tube, A, section of the sample) and the diameter d that can be directly evaluated from porosity and permeability:

$$d = \sqrt{\frac{32K}{\phi_0}} \qquad \frac{N}{A} = \frac{\phi_0^2}{8\pi K} \tag{1}$$

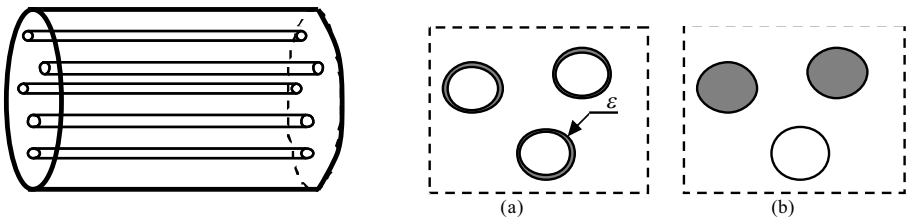

Figure 4: Schematic representation of the alteration model with two scenarios.

The drying process implies that all the salt mass remains in the porous structure. The precipitate volume of salt available is $\Omega_0 = \phi_0 AL\ Ci/\rho_s$ where ρ_s is the density of the solid salt, L the length of the sample. This added volume leads to a porosity decrease: $\delta\phi = \phi_0\ Ci/\rho_s$. We assume here that the salt volume is distributed in the porous structure through two ways. In the scenario (a), the deposition is uniform in the tubes (Figure 4(a)), in scenario (b) the pores are totally filled (Figure 4 (b)). The Poiseuille flux in remaining tubes is calculated and compared to the Darcy flux. This leads to the permeability alteration:

$$\frac{K_g^f}{K_g^i} = \left(1 - \frac{1}{2}\frac{C}{\rho_s}\right)^4 \quad \text{(a)} \qquad \frac{K_g^f}{K_g^i} = 1 - \frac{C}{\rho_s} \quad \text{(b)} \tag{2}$$

A first remark is that the linear trend is obtained only in the case of pore complete blockage by salt precipitation. The experiments suggest this alteration mode. The alterations of equations (2) were compared with the experiments (Figure 5 (a)) without agreements. The alteration is larger in reality. However the porosity decrease is well predicted by the volume balance (Figure 5 (b)).

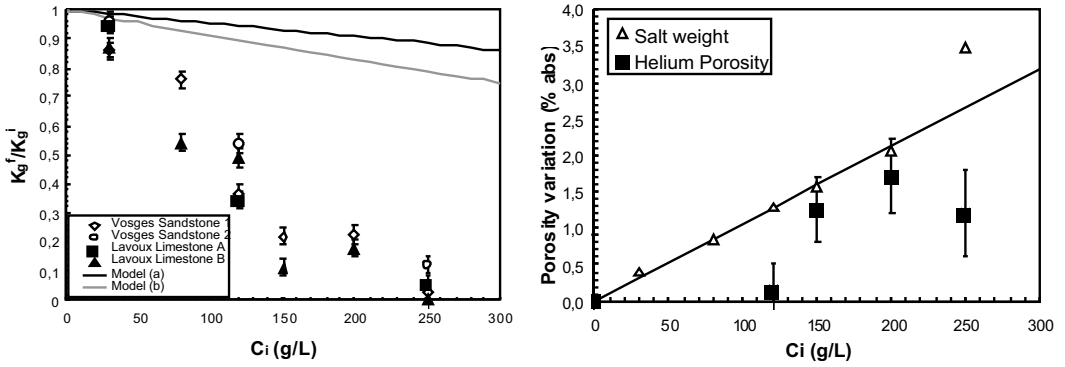

(a) (b)

Figure 5: (a) Permeability alteration and models. (b) Porosity variation in Vosges Sandtone 1.

The decrease in porosity has been measured in two independent ways. The weighing of the initial sample and after complete drying allows a very accurate measurement of the salt content. Moreover, we verified that the total amount of precipitated salt corresponded exactly to the one introduced in solution. In Figure 5 (b), we represent $(m/m_0)(\rho/\rho_s)(1-\phi_0)$ the absolute porosity variation estimated from the weighing (m added mass of salt, m_0 dry sample mass, the density of the solid salt $\rho_s=1984\ kg/m^3$ for KCl and $\rho=2661\ kg/m^3$ measured density of the sandstone) and $\delta\phi = \phi_0 Ci/\rho_s$ (black line) the porosity variation calculated from the initial salt concentration.

The porosity was also measured with a Helium porosimeter. The difficulty is that the measurement is very sensitive to any change of total volume (small edges erosion after the different experimental steps) so the error bars are quite significative, but the absolute porosity decrease is about only 1% confirming the hypothesis that precipitated salt is the only added volume. An interesting observation in Figure 5 (b) is that for the largest salt concentration, the measured mass is larger that the initial mass of salt. We interpret this observation by the fact that some water remains trapped in the porous structure, because the permeability alteration is very large as shown in Figure 1. Consequently, the porosity change measured with Helium is also less than expected.

The surprising conclusion of the comparison between the model and the experiment is that the permeability alteration is large but the porosity change moderate. We will see in the next part that this effect is due to the non-uniform distribution of the salt in the porous structure.

4. Local investigation

The key hypothesis in the alteration model is the homogeneity of the salt deposition. To check this hypothesis, we performed a 3D tomography analysis with a high resolution micro X-ray scanner. A cylindrical plug of 5 mm in diameter and 10 mm long of the Vosges sandstone 2 was initially scanned and the 3D structure was obtained. The plug is then saturated with potassium iodide (KI 80 g/L) by spontaneous imbibition, and dried with only the upper face free. At the end of the drying, the 3D structure is analyzed again.

4.1. Spatial distribution

The 3D distribution of the precipitated salt in the porous structure is shown in Figure 6. The reconstruction is

obtained with the micro X-ray scanner by substraction of the first and final state.

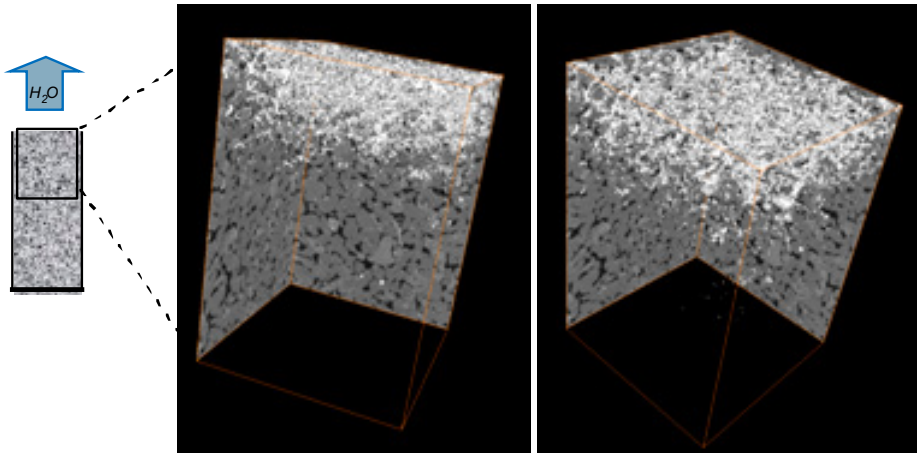

Figure 6: 3D reconstruction of the salt precipitated in Vosges Sandstone 2. The bottom plan is the upper face.

The main observation is that the salt is precipitated only in a small area just underneath the sample evaporating surface. Figure 7 has been obtained with scanning electron microscopy from a fracture plan of one of the sample used for permeability measurement (Vosges sandstones 1 prepared with 250 g/L KCl). The white zone is the solid KCl in the porosity. In the two cases, salt is localized in a small zone of about 10-20% of the total length near the evaporating surface.

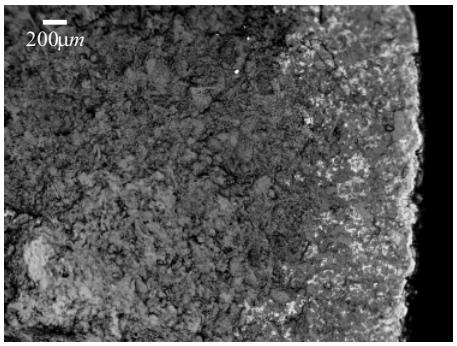

Figure 7: Precipitated salt in Vosges Sandstone 1 observed under SEM (backscattered electron).

Dissolved salt flow during the drying stage has been recently studied theoretically [8-9] and it has been shown that the exchange of water takes place at the interface and in water wet stones, capillary flows pull water to the evaporating surface. These convective brine flows accumulate salt near the surface, but as the salts do not evaporate, only Fick diffusion process counterbalances this effect and thus tend to homogenize the salt profile. These authors showed that a Peclet number (Pe) is pertinent in this situation, representing the ratio between convective flows and diffusive flows.

$$Pe = \frac{\xi L}{\rho_w \phi_0 D} \tag{3}$$

ξ is the drying rate (the mass of loss water vapor per unit surface and unit time), D the diffusion coefficient of salt in water. For large Peclet ($Pe >> 1$), the salt concentration is non homogeneous and salts accumulate near the surface, homogeneous profiles are obtained for small Peclet numbers ($Pe << 1$). By measuring the mass evolution

with time, we calculated the drying rate in our experiments. In our oven at 60°C, Pe = 70, confirming that the flow regime is convective and that salt mainly accumulates near the evaporating surface as shown in Figure 7.

4.2. Local Observation

We performed scanning electron microscopy analysis to see how salts are locally distributed within the samples used for permeability alteration measurements.

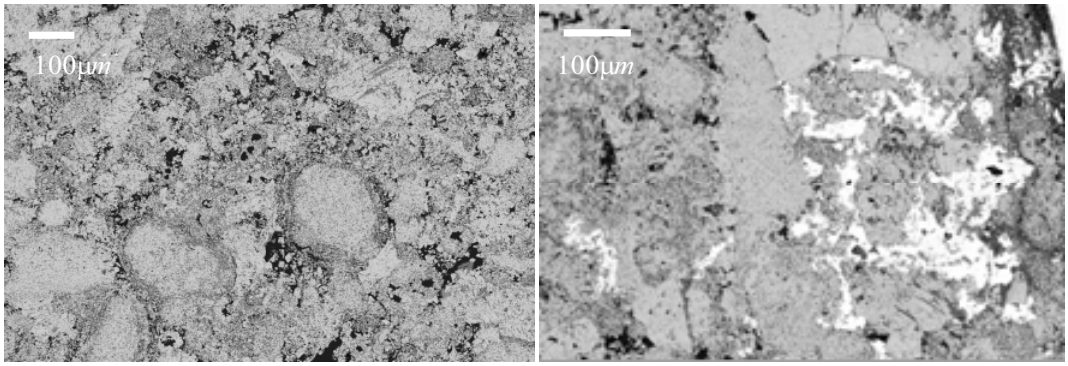

Figure 8: Lavoux Limestone B at initial dry state and after salt precipitation (SEM, backscattered electron).

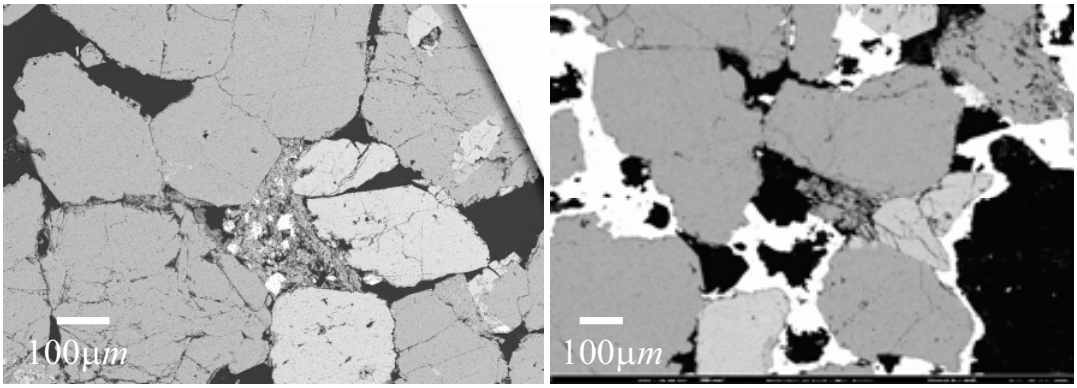

Figure 9: Vosges sandstone 2 at initial dry state and after salt precipitation (SEM, backscattered electron).

The experiments have been done with Vosges Sandtone 1 and Lavoux Limestone B, at initial conditions and after 250 g/L KCl precipitation. Figure 8 and Figure 9 show pictures before and after precipitation. We clearly see that the macro porosity is filled with white salt deposits. The solid salts are not porous and seem to mainly fill the pore throat (especially in the Limestone case). Some surface deposition can also be observed. This confirms that the main mode of alteration is like the scenario (b) used in the model.

4.3. Model update

From the observation, we modify the model saying that the salt only precipitate in a size l much smaller than the sample length L. We introduce the relative alteration size: $\zeta = l/L$ and the model with the (b) scenario becomes:

$$\frac{K'}{K} = 1 - \frac{C_i}{\zeta \rho_s} \tag{4}$$

The permeability alteration versus $C_i/\zeta\rho_s$ is represented in Figure 10 with an adjustment of ζ. In doing so, we obtain the same trend for all the experiments (salt and rock). The value of ζ is represented in Figure 10(b) and is remarkably quasi constant $\zeta \approx 16\%$. As shown by [8-9], the dissolved salt concentration profile within the porous structure is mainly controlled by the Peclet number (Pe). As this number is kept constant in our experiments, we suggest that ζ is mainly dependent on Pe. Further investigation are needed to confirm this assumption.

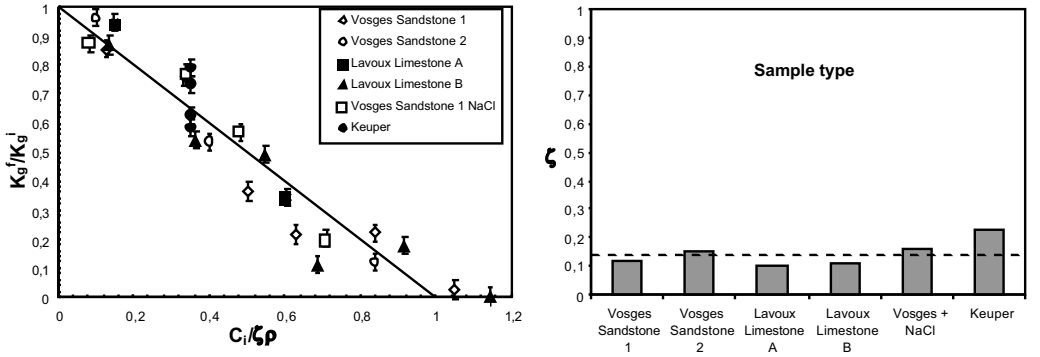

Figure 10: Left: Experimental permeability alteration for the different rock type and salt and linear trend of equation (4). Right: ζ obtained in the different situations.

5. Conclusion

Permeability alteration has been measured systematically for four type of rocks representative of aquifer storage rocks and for three types of salts. A coherent linear decrease is observed. Local investigation shows that the salt precipitation is localized near the surface of the sample and pores are blocked by solid salt precipitations. From these observations, a simple volume balance model is able to represent the trend of all the experiments.

In the case of drying by gas injection, we expect the same physical mechanisms and an accumulation of salt near the injection surface leading to permeability alteration.

Aknowledgements

This work was carried out within the framework of the ANR Proche Puits project, co-funded by the French National Agency for Research (ANR). The authors want to thank all partners to allow the publication of this work.

References

[1] Mujumbar A.S., 1992. Advances in Drying, Hemisphere Publishing Corporation

[2] Pruess K. and Müller N, 2009. Formation dry-out from CO_2 injection into saline aquifers: 1. Effects of solid precipitation and their mitigation. *Water Resources Research*, 45, W03402

[3] Giorgis T., Carpita M., Battistelli A., 2007. 2D modeling of salt precipitation during the injection of dry CO_2 in a depleted gas reservoir. *Energy Conversion and Management*, 48, 1816-1826

[4] Zeidoni M., Pooladi-Darvish M., Keith D., 2009. Analytical solution to evaluate salt precipitation during CO_2 injection in saline aquifers. *International Journal of Greenhouse Gas Control*, 3, 600-611

[5] Mahadevan J., Sharma M.M., Yortsos Y.C., 2007. Water removal from porous media by gas injection : experiments and simulation, *Trans. Porous Med.*, 66, 287-309

[6] André L., Azaroual M., Peysson Y., Bazin B., 2010. Impact of porous medium desiccation during anhydrous CO2 injection in deep saline aquifers: up scaling from experimental results at laboratory scale to near-well region. *International Conference on Greenhouse Gas Technologies* (GHGT-10), Amsterdam, 19-23 September 2010

[7] Azaroual M., Fouillac C., Matray J.M., 1997. Solubility of silica polymorphs in electrolyte solutions, II. Activity of aqueous silica and solid silica polymorphs in deep solutions from the sedimentaty Paris Basin, *Chemical Geology*, 140, 167-179

[8] Guglielmini L., Gontcharov A., Aldykiewicz Jr., Stones H.A., 2008. Drying of salt solutions in porous materials: Intermediate-time dynamics and efflorescence, *Physics of Fluids*, 20, 077101

[9] Huinink H.P., Pel L., Michels M.A.J., 2002. How ions distribute in a drying porous medium: A simple model, *Physics of Fluids*, 14-4, p 1389-1395.